Consistent description of mesoscopic transport: Case study of current-dependent magnetoconductance in single GaN:Ge nanowires

Patrick Uredat,[1,2,*] Pascal Hille,[1,2] Jörg Schörmann,[1,2] Martin Eickhoff,[3] Peter J. Klar,[1,2] and Matthias T. Elm[1,2,4,†]

[1]*Center for Materials Research (LaMa), Justus Liebig University Giessen, Heinrich-Buff-Ring 16, D-35392 Giessen, Germany*

[2]*Institute of Experimental Physics I, Justus Liebig University Giessen, Heinrich-Buff-Ring 16, D-35392 Giessen, Germany*

[3]*Institute of Solid State Physics, University of Bremen, Otto-Hahn-Allee 1, D-28359 Bremen, Germany*

[4]*Institute of Physical Chemistry, Justus Liebig University Giessen, Heinrich-Buff-Ring 17, D-35392 Giessen, Germany*

(Received 29 June 2018; revised manuscript received 12 July 2019; published 7 August 2019)

The so called phase-coherence length l_φ and its relation to the geometrical dimensions of a sample determine the electronic transport regime. Different approaches are established for extracting l_φ from magnetotransport data of mesoscopic systems and need to be cross-checked by using experimental data on the same model system in order to ensure an overall consistent theoretical description. Suitable model systems for testing this consistency are single GaN:Ge nanowires. Their magnetoconductance at low temperatures exhibits universal conductance fluctuations as well as weak localization effects. We find that the values of l_φ obtained from the established analysis of the magnitude of the conductance fluctuations rms(ΔG) decrease with increasing measurement current, whereas the corresponding values of l_φ determined by the analyses of the correlation field B_C and the weak localization effect yield the same value for l_φ independent of the measurement current used. We apply and modify the existing theoretical framework for bias-dependent differential conductance fluctuations, in order to explain the decrease of the conductance fluctuations rms(ΔG) with increasing current density in our dc measurements. This leads to the same values of l_φ independent of the analysis approach applied to the same set of data.

DOI: 10.1103/PhysRevB.100.085409

I. INTRODUCTION

To further increase the performance of semiconducting devices other materials, such as III-V semiconductors, need to be integrated onto the existing silicon technology. The integration of these materials is, among others, limited by the formation of dislocations due to the lattice mismatch with the substrate. Semiconducting nanowires overcome such limitations and beyond that provide excellent physical properties for future nanoscaled electronical devices. In particular, gallium nitride (GaN) nanowires are promising candidates for optoelectronics and high power field-effect transistors because of the direct band gap and large electron mobilities [1–4]. However, to use GaN nanowires in optical and electrical devices, a detailed understanding of the fundamental transport properties of the nanowires is needed. Although studied over the past decades the transport properties in mesoscopic systems have not yet been fully understood. Doped GaN nanowires are an ideal model system for studying the fundamental properties of mesoscopic systems such as the transition from a diffusive to a ballistic transport regime in strongly confined structures [5–10]. The character of the electronic transport is determined by the interplay of different length scales. These are, on the one hand, geometrical extensions of the system and, on the other hand, lengths characteristic for the scattering mechanisms occurring in the system. One of the latter is the so called phase-coherence length l_φ, i.e., the characteristic length over which the electron phase is preserved [11–14]. If the phase-coherence length is comparable to the system's geometrical extensions, quantum interference effects can be directly observed. Universal conductance fluctuations (UCF) and weak localization (WL) are two prominent examples of such quantum interference phenomena [15–18]. The phase-coherence length may be determined by three different approaches when analyzing the magnetotransport measurements [10,12,19], i.e., (i) by evaluation of the magnitude of the conductance fluctuations rms(ΔG), (ii) by the correlation field B_C, or (iii) by the weak localization effect. All three approaches must yield the same value for l_φ to give a consistent description [7,10,20]. Performing a careful analysis of magnetotransport data of single Ge-doped GaN nanowires, we demonstrate that based on the existing models this is not the case. The l_φ values based on approach (i) deviate from those of the other two approaches due to an alleged reduction of rms(ΔG), in particular, as a function of current density or applied electric field.

A bias dependence of differential conductance fluctuations δG^d [not to be confused with rms(ΔG)] was first theoretically predicted by Larkin and Khmel'nitski [21] and experimentally observed in metallic nanowires and rings [22–25], as well as in metal-oxide-semiconductor field-effect transistors [26]. The differential conductance fluctuations increase in these systems with increasing bias voltage at first and then start to decrease again. The decrease of δG^d at sufficiently high voltages V is explained by a reduction of the phase-coherence

*patrick.uredat@physik.uni-giessen.de

†matthias.elm@exp1.physik.uni-giessen.de

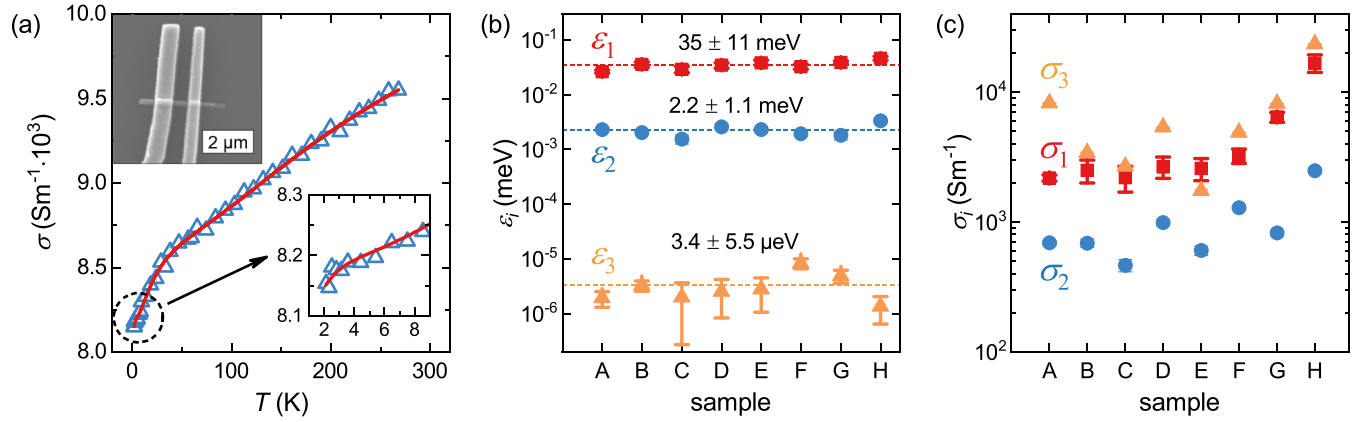

FIG. 1. (a) Measured temperature-dependent conductivity of nanowire A (blue triangles) and theoretical model (red solid line). The inset shows exemplarily an SEM image of a contacted nanowire sample. (b) Determined activation energies ε_1, ε_2, ε_3 for samples A–H. (c) Determined conductivities σ_1, σ_2, σ_3 for samples A–H.

length by inelastic scattering, in agreement with theory [21,27]. In this context V denotes the voltage drop per coherence length l_φ and $E_c = \hbar D/l_\varphi^2$ is the so called Thouless energy and D the diffusion coefficient of electrons. However, such a behavior is only observed for the differential conductance measured in ac lock-in technique, where $eV \gg E_c, k_B T$. Here, we report on voltage-dependent magnetoconductance fluctuations measured in a dc bias technique in a regime $eV_{dc} \approx E_c \approx k_B T$. We explain the reduction of the magnitude of UCF rms(ΔG) with V_{dc} by electric-field averaging of uncorrelated energy intervals somewhat similar to the thermal averaging derived by Lee, Stone, and Fukuyama, which explains the reduction of rms(ΔG) with increasing temperature [28]. The proof that the reduction of rms(ΔG) is not caused by a reduction of l_φ due to inelastic scattering is possible only because, for the mesoscopic system under study, values of l_φ can be determined independently by three different methods from the same magnetoresistance curves.

II. EXPERIMENTAL METHODS

Self-assembled Ge-doped GaN nanowires were grown in nitrogen-rich conditions on Si(111) substrates at temperatures of 795 °C using plasma-assisted molecular beam epitaxy (PAMBE) [29]. The growth conditions yielded doped GaN nanowires with an effective carrier concentration in the order of 2 to 4 × 10^{19} cm^{-3} determined by Seebeck measurements [10,30]. Structural analysis of the nanowires with a scanning electron microscope (SEM) revealed an average length of about 1.5 to 2.0 μm and a diameter d between 60 and 140 nm. The GaN nanowires were detached from the substrate by sonication and transferred to an oxidized Si(100) substrate in order to separate them and to contact individual specimens. The electrical contacts were prepared by a combination of photo- and electron-beam lithography. Ohmic contacts were realized by thermally depositing 25 nm Ti followed by 200 nm Au onto the designated contact areas and annealing of the sample at 600 °C for 60 s in high vacuum.

Magnetotransport measurements at various temperatures were carried out using a He-4 flow cryostat with a superconducting magnet system providing external fields up to 10 T. The nanowire axis was oriented perpendicular to the external magnetic field. dc currents ranging from 100 to 1500 nA have been applied to measure the magnetoresistance in two-probe geometry. For each current and at each magnetic field value, the voltage drop was averaged 20 times with a Keithley Nanovoltmeter 2182. The two-probe geometry was used to ensure the symmetry of the magnetoresistance under magnetic field reversal [6]. We averaged the conductance data for positive and negative magnetic field to reduce the influence of noise. The typical two-point resistance for different samples varied between 4000 and 9000 Ω at room temperature. The electrical conductivity was calculated assuming a cylindrical shape of the nanowire and using the geometrical parameters determined by SEM.

III. RESULTS AND DISCUSSION

We investigated the temperature dependence of the conductivity of eight Ge-doped GaN nanowires (samples A–H) in the temperature range between 1.7 and 280 K. Figure 1(a) exemplarily shows the temperature dependence of the conductivity of nanowire A. As the conductivity decreases with decreasing temperature, the Ge-doped GaN nanowire exhibits a semiconducting behavior. The temperature dependence of the conductivity of such a nanowire is affected by three different transport processes, namely the thermal excitation of electrons from the impurity band to the conduction band at high temperatures, the conduction of electrons via neutral donors at intermediate temperatures, and a conduction within the impurity band at low temperatures. Taking all three transport processes into account the temperature dependence of the conductivity can be expressed as [31]

$$\sigma(T) = \sigma_1 e^{-\varepsilon_1/k_B T} + \sigma_2 e^{-\varepsilon_2/k_B T} + \sigma_3 e^{-\varepsilon_3/k_B T}, \qquad (1)$$

where the activation energies ε_1, ε_2, ε_3 and the conductivities σ_1, σ_2, σ_3 are associated with these three transport processes, respectively. According to theory the relations $\varepsilon_1 > \varepsilon_2 > \varepsilon_3$ and $\sigma_1 \gg \sigma_2 \gg \sigma_3$ should hold [31]. The activation energies and the corresponding conductivities of samples A to H are shown in Figs. 1(b) and 1(c), respectively. All measured samples A to H exhibit comparable values for each of the

three activation energies. The mean value for the activation energy ε_1 corresponding to carrier activation from the donor level into the conduction band is 35 ± 11 meV. It should be noted that a reasonable agreement between the activation energy ε_1 of the different nanowires is achieved only if all three transport processes are considered. The mean value is in good agreement with the theoretically predicted ionization energy of a Ge donor in GaN of $E_{\text{ion}}^{\text{Ge}} \approx 31$ meV [32]. Corresponding experimental values in the range from 19 to 50 meV have been reported in literature [33,34]. Furthermore, the activation energy $\varepsilon_2 = 2.2 \pm 1.1$ meV is approximately one-tenth of the ε_1 and, thus, also in agreement with the theoretical expectations. The mean value of the activation energy $\varepsilon_3 = 3.4 \pm 5.5$ μeV, which is characteristic for the conduction in an impurity band at temperatures below 10 K [35], is much smaller, again in accordance with theory. However, the corresponding conductivity values do not quite fulfill the relation $\sigma_1 \gg \sigma_2 \gg \sigma_3$, in particular, σ_3 is much larger than expected. We attribute this deviation to the vicinity of the insulator-to-metal transition. The conduction in the impurity band at these low temperatures is in the metallic regime, i.e., carried by delocalized electrons. In this metallic transport regime the mobility of carriers and thus the conductivity is significantly larger than in case of the insulating regime where transport takes place by hopping of localized electrons between impurity states.

Magnetotransport measurements of nanowires A and B were performed for various current densities at a constant temperature of 1.7 K. As recently shown, slightly doped GaN:Ge nanowires show a quasi-one-dimensional transport bahavior [10], i.e., l_φ is smaller or comparable to the diameter of the nanowire, whereas the diffusive transport remains in the weakly disordered regime (dirty metal limit, $l \ll d$, with the mean free path l). The change of the magnetoconductance with magnetic field $\Delta G(B)$ was extracted from the magnetoresistance data using [10,36]

$$\Delta G(B) = G(B) - \langle G(B) \rangle \cong -\frac{\Delta R(B)}{\langle R(B) \rangle_B^2}, \tag{2}$$

where $\langle R(B) \rangle_B$ is the mean resistance averaged over the full magnetic field range and $\Delta R(B) = R(B) - \langle R(B) \rangle_B$ denotes the fluctuations of the resistance. Both nanowires show a negative magnetoresistance effect, i.e., a positive magnetoconductance effect, for magnetic fields below 1 T due to WL. This effect is accompanied by UCF with an amplitude of a few tenths of e^2/h [Figs. 3(a) and 3(d)], which are observable up to 10 T. The weak localization effect (WL) arises from enhanced backscattering of electrons in the absence of a magnetic field due to a constructive interference of the electron paths induced by time reversal symmetry [12]. The latter is broken by applying a magnetic field. The corresponding backscattering of electrons is no longer enforced and, thus, the conductivity increases with increasing magnetic field. The UCF in strongly confined systems, on the other hand, are caused by the interference of different coherent electron transport paths forming loops [37,38]. The magnetic flux through such a loop changes when the external magnetic field is varied. This flux variation in turn alters the electron interference and the UCF emerge. The presence of WL and UCF in the measured magnetoconductance curves confirms that the transport properties of the nanowires are mesoscopic. It implies that l_φ is comparable to the diameter of the nanowire and larger than l_e, which is the distance between elastic scattering centers, i.e., donors or sidewalls.

Three different approaches for determining the phase-coherence length l_φ are established for mesoscopic systems. Approach (i) analyzes the root mean square of the conductance fluctuations rms(ΔG). If l_φ is smaller than the length of the nanowire L between the two voltage probes rms(ΔG) is given by [11,12,16]

$$\text{rms}(\Delta G) \propto \frac{e^2}{h}\left(\frac{l_\varphi}{L}\right)^{3/2}. \tag{3}$$

In approach (ii), l_φ is determined from an analysis of the correlation field B_{C}, which represents a characteristic field period of the conductance fluctuations. The correlation field B_{C} is defined by the autocorrelation function $F(B_{\text{C}}) = 1/2F(0)$, where $F(\Delta B) = \langle \Delta G(B + \Delta B) \Delta G(B) \rangle_B$ [38,39]. The phase-coherence length is estimated from the correlation field using $B_{\text{C}} = \gamma\, \Phi_0/l_\varphi d$, where d denotes the diameter of the nanowire and $\gamma = 0.42$ [40]. Approach (iii) makes use of the weak localization effect. In the case of quasi-one-dimensional transport in a weakly disordered regime, the phase coherence can be obtained from the WL magnetoconductance at low magnetic fields [10–12]:

$$\Delta G(B) = -\frac{2}{L}\frac{e^2}{h}\left[\frac{1}{l_\varphi^2} + \frac{1}{3}\frac{d^2 e^2 B^2}{\hbar^2}\right]^{-1/2}. \tag{4}$$

Figure 2(b) shows exemplarily the magnetoconductance correction due to the weak localization effect for sample A for various temperatures at low magnetic fields. The solid lines represent the fits based on the theoretical model for the one-dimensional weak localization effect [40]. The small modulations arise from the UCF which are also present in this magnetic field range. The extracted phase-coherence lengths l_φ^{WL} for temperatures between 2 and 40 K are depicted in Fig. 2(c) for samples A and H. The decrease of the phase-coherence lengths with increasing temperature is proportional to $\sim T^{-0.20}$ and $\sim T^{-0.23}$ for samples A and H, respectively. Thus the nanowires show a slightly weaker temperature dependence of l_φ than the $T^{-1/3}$ law predicted by theory [11], which is typically observed for quasi-one-dimensional transport in semiconducting nanowires [5,7,9,10,20,41]. Figures 3(a) and 3(d) show the magnetotransport measurements for various measurement currents of nanowires A and B, respectively. The amplitude of the UCF decreases with increasing measurement current, whereas the pattern of the conductance fluctuations, and hence the correlation field B_{C}, does not change significantly. Also, the reduced conductance at small magnetic fields due to the weak localization effect is not affected by increasing measurement currents. The phase-coherence lengths l_φ determined by the three approaches are plotted as a function of the applied current on a double-logarithmic scale in Figs. 3(b) and 3(e). At low currents a good agreement between the values of l_φ determined by the three approaches is obtained. However, while $l_\varphi^{B_{\text{C}}}$ and l_φ^{WL} are independent of the applied current, the value of l_φ^{rms} decreases with increasing current. It should be noted that the phase-coherence length is solely determined by inelastic

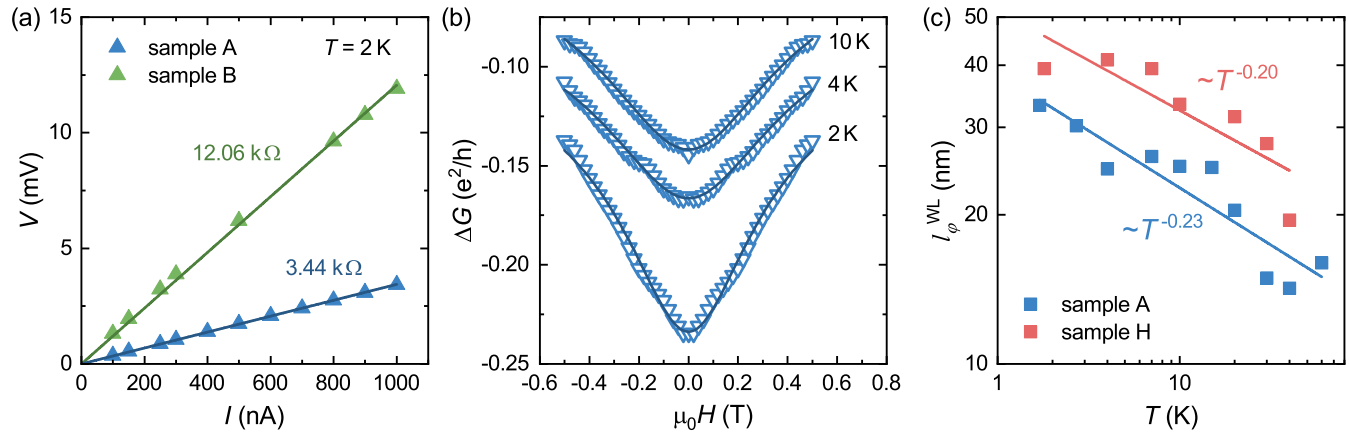

FIG. 2. (a) Current-voltage characteristic for samples A and B. (b) Magnetoconductance correction due to the weak localization effect for sample A for various temperatures at low magnetic fields. The solid lines represent the fits according to Eq. (4) for one-dimensional transport. (c) Extracted phase-coherence length l_φ^{WL} in a temperature range between 1.7 and 40 K.

scattering events, i.e., if an electron scatters inelastically, phase coherence will be lost. As the occurrence of inelastic scattering events is independent of the applied current in the investigated transport regime (i.e., $eV \approx E_c \approx k_{\mathrm{B}}T$), phase coherence should also be independent of current. This statement is in accordance with the constant values of $l_\varphi^{B_{\mathrm{C}}}$

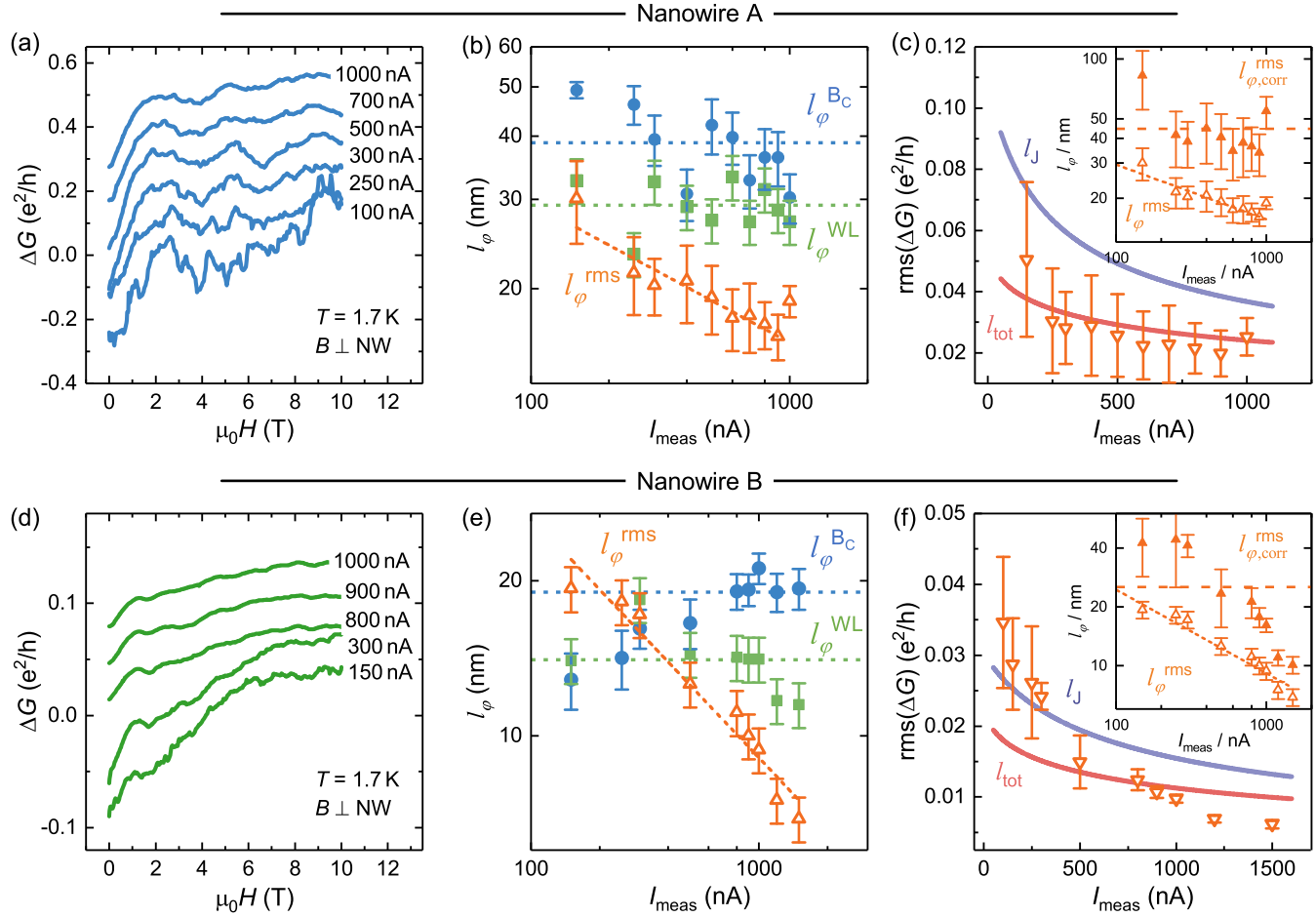

FIG. 3. (a) Magnetoconductance of nanowire A for measurement currents between 100 nA and 1000 nA. (b) Phase-coherence lengths l_φ determined by the three approaches. (c) Measured values of rms(ΔG) as a function of current and theoretical predicted decay of the rms values for nanowire A. The inset shows the values $l_{\varphi,\mathrm{corr}}^{\mathrm{rms}}$ obtained for l_φ^{rms} using our revised theoretical description. (d)–(f) Corresponding results for nanowire B.

and l_φ^{WL} within the experimental uncertainty for the current range studied, but not with a decreasing l_φ^{rms}. Furthermore, l_φ determined by all three approaches should decrease with increasing temperature in the same manner as shown by us for similar nanowire samples [10]. Thus the decrease of the phase-coherence length l_φ^{rms} with increasing I_{meas} cannot be due to Joule heating, i.e., as, for example, l_φ^{WL} decreases with increasing T as shown for samples A and H in Fig. 2(c), but is independent of I_{meas} in Figs. 3(b) and 3(e). The same holds for l_φ^{Bc}.

In the following, we explain which mechanism needs to be included to the existing description of approach (i) in order to achieve agreement with the other two approaches for extracting l_φ, i.e., to avoid the alleged reduction of the phase-coherence length l_φ^{rms} with increasing current in the analysis of the experimental data. If V_{dc} is the applied bias voltage for a system where $l_\varphi > L$ and temperature broadening is negligible, the number of uncorrelated energy intervals that contribute to the electron transport will be given by $N = V_{\mathrm{dc}}/V_{\mathrm{c}}$, with the correlation energy $E_c = eV_{\mathrm{c}} = \hbar D/l_\varphi^2$. Each energy interval contributes to the fluctuations by an amount $\sim(e^2/h)V_{\mathrm{c}}$ [24]. Therefore, the current is a random function of the applied voltage V_{dc} [21]:

$$I_{\mathrm{dc}} = \langle I\rangle + \Delta I_{\mathrm{dc}} \cdot \delta\alpha, \tag{5}$$

where ΔI_{dc} is the amplitude of the correction to the classical Ohmic current $\langle I\rangle$ and $\delta\alpha$ is a random function of V_{dc} with $\mathrm{rms}(\delta\alpha) = 1$. Larkin and Khmel'nitski derived the amplitude as $\Delta I_{\mathrm{dc}} \sim (e^2/h)(V_{\mathrm{dc}}V_c)$ [21]. Thus the total conductance G is given by

$$G = \frac{I_{\mathrm{dc}}}{V_{\mathrm{dc}}} = \frac{\langle I\rangle}{V_{\mathrm{dc}}} + \frac{\Delta I_{\mathrm{dc}}}{V_{\mathrm{dc}}} \cdot \delta\alpha \tag{6}$$

$$= \langle G\rangle + \frac{e^2}{h}\left(\frac{V_{\mathrm{dc}}}{V_c}\right)^{-1/2} \cdot \delta\alpha. \tag{7}$$

According to the second term on the right hand side one obtains that the magnitude of the conductance fluctuations $\mathrm{rms}(\Delta G)$ decreases with increasing bias voltage, i.e., with the number of uncorrelated energy intervals N, assuming that V_{dc} is larger than V_c:

$$\mathrm{rms}(\Delta G) \propto \frac{e^2}{h}\left(\frac{V_{\mathrm{dc}}}{V_c}\right)^{-1/2}. \tag{8}$$

We discuss a system with a phase-coherence length l_φ smaller than the systems length L. Thus we can consider the system to be divided into a series of L/l_φ uncorrelated segments of length l_φ, each with a voltage drop per segment of $V_{\mathrm{dc}}^{\mathrm{in}}$. The voltage drop over the entire system is then given by $V_{\mathrm{dc}} = V_{\mathrm{dc}}^{\mathrm{in}} \cdot L/l_\varphi$. According to Beenakker and van Houten [12] the conductance fluctuations of a series of independently fluctuating segments is given by $\mathrm{rms}(\Delta G) \propto (l_\varphi/L)^{3/2} \cdot \mathrm{rms}(\Delta G_1)$, where $\mathrm{rms}(\Delta G_1)$ are the root mean square of conductance fluctuations of a single segment. In the regime described above, every segment of length l_φ fluctuates independently with $\mathrm{rms}(\Delta G_1) \propto (e^2/h)(V_{\mathrm{dc}}^{\mathrm{in}}/V_c)^{-1/2}$. Consequently, the magnitude of the conductance fluctuations $\mathrm{rms}(\Delta G)$ of the entire system scales as

$$\mathrm{rms}(\Delta G) \propto \frac{e^2}{h}\left(\frac{l_\varphi}{L}\right)^{3/2}\left(\frac{V_{\mathrm{dc}}^{\mathrm{in}}}{V_c}\right)^{-1/2} \tag{9}$$

$$\propto \frac{e^2}{h}\left(\frac{l_\varphi}{L}\right)^{3/2}\left(\frac{\hbar D}{e\, l_\varphi^2\, V_{\mathrm{dc}}^{\mathrm{in}}}\right)^{1/2} \tag{10}$$

$$\propto \frac{e^2}{h}\frac{l_\varphi^{1/2}\, l_J}{L^{3/2}} \quad (l_J \ll l_\varphi). \tag{11}$$

Here, we propose a current length scale $l_J = \sqrt{\hbar D/eV_{\mathrm{dc}}^{\mathrm{in}}}$, where $D = \hbar^2(3\pi^2 n)^{2/3}\mu/(3\, m_e\, e)$ is the diffusion constant, in analogy to the thermal length l_T proposed by Lee, Stone, and Fukuyama [28], who described the influence of finite temperature on the $\mathrm{rms}(\Delta G)$ in a similar fashion. At finite temperatures, the energy range $k_{\mathrm{B}}T$ around the Fermi energy divides into $k_{\mathrm{B}}T/V_c$ uncorrelated energy intervals leading to this averaging effect and thus to less pronounced UCF at higher temperatures. Lee *et al.* included this effect in the theoretical description of $\mathrm{rms}(\Delta G)$ by introducing the thermal length $l_T = \sqrt{\hbar D/k_{\mathrm{B}}T}$ [12,28]. This is the length two interfering electron paths traverse with the energy difference $\Delta E = k_{\mathrm{B}}T$ until they have to be considered uncorrelated [12]. Taking this thermal averaging into account for an intermediate regime (where $l_T \approx l_\varphi$) $\mathrm{rms}(\Delta G)$ is given by an interpolation formula

$$\mathrm{rms}(\Delta G) = \alpha\, \frac{e^2}{h}\left(\frac{l_\varphi}{L}\right)^{3/2}\left[1 + \beta\left(\frac{l_\varphi}{l_T}\right)^2\right]^{-1/2}, \tag{12}$$

with $\alpha = \sqrt{6}$ and $\beta = 9/2\pi$. In order to explain the reduction of the phase-coherence length l_φ^{rms} with increasing current density for a similar regime where $l_J, l_T \approx l_\varphi$, that is $eV_{\mathrm{dc}}^{\mathrm{in}} \approx E_c \approx k_{\mathrm{B}}T$ (see also Table I.), we modified the existing formula (12) to account for both effects in the intermediate regime:

$$\mathrm{rms}(\Delta G) = \alpha\, \frac{e^2}{h}\left(\frac{l_\varphi}{L}\right)^{3/2}\left[1 + \beta\left(\frac{l_\varphi}{l_{\mathrm{tot}}}\right)^2\right]^{-1/2}, \tag{13}$$

with $l_{\mathrm{tot}}^{-1} = l_T^{-1} + l_J^{-1}$. The $\mathrm{rms}(\Delta G)$ values of the conductance fluctuations at 1.7 K of nanowires A and B are plotted in Figs. 3(c) and 3(f), respectively. The solid lines represent the modeling of the current dependence of $\mathrm{rms}(\Delta G)$ using Eq. (13) with the above given l_{tot} as well as with $l_{\mathrm{tot}} = l_J$ only, where thermal averaging was neglected. For nanowire A, the modeled curve with $l_{\mathrm{tot}}^{-1} = l_T^{-1} + l_J^{-1}$ is in good agreement with the experimentally determined $\mathrm{rms}(\Delta G)$ values, which indicates that both thermal averaging and bias induced averaging need to be considered for nanowire A at 1.7 K. For nanowire B, the experimentally determined $\mathrm{rms}(\Delta G)$ values are for small current densities in good agreement with the modeled curve for $l_{\mathrm{tot}} = l_J$ and for higher current densities

TABLE I. Overview of important experimental parameters for samples A and B.

Sample	L (nm)	d (nm)	$R_{\mathrm{RT}}^{\mathrm{2P}}$ (kΩ)	$n/10^{18}$ (cm^{-3})	μ ($\mathrm{cm}^2\mathrm{V}^{-1}\mathrm{s}^{-1}$)	D ($\mathrm{cm}^2\mathrm{s}^{-1}$)	l_e (nm)	l_T^{2K} (nm)	$l_J^{1\mu\mathrm{A}}$ (nm)
A	401	135	2.94	5.85	78	3.07	2.85	37.1	21.6
B	375	90	10.60	3.00	78	1.94	2.26	29.5	14.3

in good agreement with the curve for $l_{\mathrm{tot}}^{-1} = l_T^{-1} + l_J^{-1}$. The thermal length l_{T} is about 37.1 and 29.5 nm for nanowires A and B, respectively. The lengths l_J for nanowire A range from 55.8 to 21.6 nm and for nanowire B from 36.9 to 14.3 nm for applied currents of 150 to 1000 nA, respectively. (See also Table I.)

The phase-coherence length $l_{\varphi,\mathrm{corr}}^{\mathrm{rms}}$ as a function of current obtained using Eq. (13) with $l_{\mathrm{tot}}^{-1} = l_T^{-1} + l_J^{-1}$ are shown in the insets of Figs. 3(c) and 3(f). Although the values of $l_{\varphi,\mathrm{corr}}^{\mathrm{rms}}$ show some random fluctuations, they are to a good approximation constant within the range of currents applied and in good agreement with l_φ^{WL} and $l_\varphi^{B_{\mathrm{C}}}$. Furthermore, the carrier concentration n and mobility μ obtained from the theoretical model [Eq. (13)] are in good agreement with those determined by Seebeck measurements as reported previously [10]. For both nanowires, a mobility of about 78 $\mathrm{V\,s/cm^2}$ was determined, while a carrier concentration of 5.85×10^{18} cm^{-3} and 3.00×10^{18} cm^{-3} was obtained for nanowires A and B, respectively. These values result in a conductivity of 7507 $\mathrm{S\,m}^{-1}$ for nanowire A and 3005 $\mathrm{S\,m}^{-1}$ for nanowire B, which are in good agreement to the measured conductivities at low temperatures.

IV. CONCLUSION

We demonstrate the reduction of the magnitude of universal conductance fluctuations rms(ΔG) with increasing current density in nanowires. The bias-induced reduction of the UCF amplitude is attributed to an increased number of uncorrelated energy intervals contributing to the electron transport at high current densities. Introducing a current-dependent length scale l_J in analogy to the thermal length l_T proposed by Lee *et al.* allows us to modify the theoretical analysis of rms(ΔG) such that the extracted phase-coherence lengths are in agreement with those extracted by other methods from the same set of magnetoresistance data. Having achieved this consistent description, this also offers a way of determining or verifying carrier concentration and carrier mobility data of mesoscopic semiconducting nanowires at low temperatures.

ACKNOWLEDGMENTS

The authors would like to thank C. Heiliger for fruitful discussions. P.U., P.J.K., and M.T.E. gratefully acknowledge financial support of the DFG via the Project No. EL 863/4-1 (367007721).

[1] M. Nami, I. E. Stricklin, K. M. DaVico, S. Mishkat-Ul-Masabih, A. K. Rishinaramangalam, S. R. Brueck, I. Brener, and D. F. Feezell, Sci. Rep. **8**, 501 (2018).
[2] X. Duan, Y. Huang, Y. Cui, J. Wang, and C. M. Lieber, Nature (London) **409**, 66 (2001).
[3] X. Duan, Y. Huang, R. Agarwal, and C. M. Lieber, Nature (London) **421**, 241 (2003).
[4] S. Li and A. Waag, J. Appl. Phys. **111**, 071101 (2012).
[5] C. Blömers, M. I. Lepsa, M. Luysberg, D. Grützmacher, H. Lüth, and T. Schäpers, Nano Lett. **11**, 3550 (2011).
[6] R. Frielinghaus, S. E. Hernández, R. Calarco, and T. Schäpers, Appl. Phys. Lett. **94**, 252107 (2009).
[7] S. Alagha, S. E. Hernández, C. Blömers, T. Stoica, R. Calarco, and T. Schäpers, J. Appl. Phys. **108**, 113704 (2010).
[8] S. Estévez Hernández, M. Akabori, K. Sladek, C. Volk, S. Alagha, H. Hardtdegen, M. G. Pala, N. Demarina, D. Grützmacher, and T. Schäpers, Phys. Rev. B **82**, 235303 (2010).
[9] A. E. Hansen, M. T. Björk, I. C. Fasth, C. Thelander, and L. Samuelson, Phys. Rev. B **71**, 205328 (2005).
[10] M. T. Elm, P. Uredat, J. Binder, L. Ostheim, M. Schäfer, P. Hille, J. Müßener, J. Schörmann, M. Eickhoff, and P. J. Klar, Nano Lett. **15**, 7822 (2015).
[11] J. J. Lin and J. P. Bird, J. Phys.: Condens. Matter **14**, R501 (2002).
[12] C. W. J. Beenakker and H. van Houten, Solid State Phys. **44**, 1 (1991).
[13] B. L. Altshuler, A. G. Aronov, and D. E. Khmelnitsky, J. Phys. C: Solid State **15**, 7367 (1982).
[14] D. E. Khmel'nitskii, Physica B+C **126**, 235 (1984).
[15] P. W. Anderson, E. Abrahams, and T. V. Ramakrishnan, Phys. Rev. Lett. **43**, 718 (1979).
[16] P. A. Lee, Physica A **140**, 169 (1986).
[17] H. van Houten, B. J. van Wees, M. G. J. Heijman, and J. P. André, Appl. Phys. Lett. **49**, 1781 (1986).
[18] W. J. Skocpol, P. M. Mankiewich, R. E. Howard, L. D. Jackel, D. M. Tennant, and A. D. Stone, Phys. Rev. Lett. **56**, 2865 (1986).
[19] G. Bergmann, Phys. Rep. **107**, 1 (1984).
[20] D. Lucot, F. Jabeen, M. R. Ramdani, G. Patriarche, G. Faini, D. Mailly, and J.-C. Harmand, J. Cryst. Growth **378**, 546 (2013).
[21] A. I. Larkin and D. E. Khmel'niskii, Zh. Eksp. Teor. Fiz. **91**, 1815 (1986) [Sov. Phys. JETP **64**, 1075 (1986)].
[22] R. A. Webb, S. Washburn, and C. P. Umbach, Phys. Rev. B **37**, 8455 (1988).
[23] R. Schäfer, K. Hecker, H. Hegger, and W. Langheinrich, Phys. Rev. B **53**, 15964 (1996).
[24] C. Terrier, D. Babić, C. Strunk, T. Nussbaumer, and C. Schönenberger, Europhys. Lett. **59**, 437 (2002).
[25] R. Häussler, H. B. Weber, and H. v. Löhneysen, J. Low Temp. Phys. **118**, 467 (2000).
[26] S. B. Kaplan, Phys. Rev. B **38**, 7558 (1988).
[27] T. Ludwig, Y. M. Blanter, and A. D. Mirlin, Phys. Rev. B **70**, 235315 (2004).
[28] P. A. Lee, A. D. Stone, and H. Fukuyama, Phys. Rev. B **35**, 1039 (1987).

[29] J. Schörmann, P. Hille, M. Schäfer, J. Müßener, P. Becker, P. J. Klar, M. Kleine-Boymann, M. Rohnke, M. de la Mata, J. Arbiol, D. M. Hofmann, J. Teubert, and M. Eickhoff, J. Appl. Phys. **114**, 103505 (2013).

[30] M. Schäfer, M. Günther, C. Länger, J. Müßener, M. Feneberg, P. Uredat, M. T. Elm, P. Hille, J. Schörmann, J. Teubert, T. Henning, P. J. Klar, and M. Eickhoff, Nanotechnol. **26**, 135704 (2015).

[31] B. Shklovskii and A. Efros, in *Electronic Properties of Doped Semiconductors*, edited by M. Cardona, P. Fulde, and H.-J. Queisser (Springer-Verlag, Berlin, Heidelberg GmbH, 1984), Vol. 45.

[32] H. Wang and A.-B. Chen, J. Appl. Phys. **87**, 7859 (2000).

[33] W. Götz, R. S. Kern, C. H. Chen, H. Liu, D. A. Steigerwald, and R. M. Fletcher, Mater. Sci. Eng. B **59**, 211 (1999).

[34] X. Zhang, P. Kung, A. Saxler, D. Walker, T. Wang, and M. Razeghi, Acta Phys. Pol. A **88**, 601 (1995).

[35] H. Fritzsche and M. Cuevas, Phys. Rev. **119**, 1238 (1960).

[36] E. Scheer, H. v. Löhneysen, and H. Hein, J. Vac. Sci. Technol., A **12**, 3171 (1994).

[37] B. Altshuler, Pis'ma Zh. Eksp. Teor. Fiz. **41**, 530 (1985) [JETP Lett. **41**, 648 (1985)].

[38] P. A. Lee and A. D. Stone, Phys. Rev. Lett. **55**, 1622 (1985).

[39] S. Washburn and R. A. Webb, Rep. Prog. Phys. **55**, 1311 (1992).

[40] C. W. J. Beenakker and H. van Houten, Phys. Rev. B **37**, 6544 (1988).

[41] Y. Niimi, Y. Baines, T. Capron, D. Mailly, F.-Y. Lo, A. D. Wieck, T. Meunier, L. Saminadayar, and C. Bäuerle, Phys. Rev. B **81**, 245306 (2010).